EXPERIMENTAL INVESTIGATION AND CFD ANALYSIS OF A Y-FRACTAL MICROCHANNEL BASED HEAT SINK

H. WU[1,*], R. KWATRA[1], M. MIRZAEIAN[1], X. LIU[1,2], J. GRANT[1]

1. [*]Institute of Engineering and Energy Technologies, School of Engineering and Computing, University of the West of Scotland, Paisley, United Kingdom; Email: Hongwei.wu@uws.ac.uk
2. Faculty of Material and Energy, Guangdong University of Technology, Guangzhou, 510006, China

Abstract

In this article, a combined experimental and computational study has been conducted to provide better understanding of the flow and heat transfer in a Y-fractal microchannel. A new test rig was set up to investigate the effect of three different control factors, i.e., fluid flow rate, inlet temperature and heat flux, on the heat transfer characteristics of the microchannel. A standard k-ε turbulence CFD model was developed, validated and employed to simulated the flow and heat transfer microchannel. Furthermore, an improved new design was suggested to further increase the heat transfer performance and create uniformity of temperature distribution.

Keywords: Heat Transfer, Microchannel, Heat Sink, CFD

1 INTRODUCTION

Miniaturization of electronic devices has led to advances in various engineering fields, including space technology, defense systems, aerospace applications, manufacturing technology, industrial processes and consumer electronics [1]. Heat dissipation in the electronic components, however, is being a critical issue due to the faster increase in the components' heat flux and increasing demand for the miniature in features' size. The heat flux of the electronic chips may exceed 400 W/cm^2 in order to meet the demand for high performance electronic components. Since overheating of the electronic components degrades the components' performance, reliability and even cause failure of the components, high performance cooling techniques are required to keep device temperatures low for acceptable performance and reliability [2-5].

The microchannel heat sink (MCHS) is a concept well suited for many electronic applications because of its ability to remove a large amount of heat from a small area [6]. Many studies have been devoted to the fluid flow and heat transfer in microchannel over the past decades. A review of the fundamental investigations relevant to the single-phase convective heat transfer in microchannels can be traced back to Morini [7]. In a recent study, a comprehensive review has been performed on single and two-phase microchannels [8]. This review looks into the difference methodologies and correlations used to predict the heat transfer and pressure drop characteristics of microchannels along the channel geometries and flow regimes. Li et al. [9] presented a series of microchannel heat sinks with Y-shaped bifurcation that were designed based on the rectangular straight microchannel heat sink, and the heat transfer and pressure drop characteristics for all cases were analysed. It was concluded that the Y-shaped bifurcation plates placed in water-cooled microchannel heat sinks could improve the overall thermal performance when the angle between the two arms of the Y-shaped plates is designed properly. According to the numerical analysis by Zhang et al. [10], measurement of accurate pressure drop in MCHS is still very difficult. But it is clearly proven that joins and bends in a fractal microchannel design result in a higher heat transfer coefficient and a more effective cooling device. Zhang et al. [11,12] also proved the relation between Reynolds number and aspect ratio on vorticity and further the effect on heat transfer. Xu et al. [13] also showed distributions of pressure drop, Nusselt number and temperature effects on silicon MCHS for various pulsation frequencies and its enhanced cooling capacity. A maximum of 47% of enhancement in heat transfer was also observed by Lee et al. [14] as a result of introduction of fins in the geometry.

Although many significant results in the flow and heat transfer characteristics of microchannel have already been obtained, the comprehension of the flow and heat transfer mechanism of Y-fractal microchannel is still quite limited. The present work aims to investigate the flow and heat transfer in Y-fractal microchannel both experimentally and numerically. Further calculation based on the validated CFD model on a new type of microchannel is numerically well demonstrated.

2 EXPERIMENTAL AND COMPUTATIONAL METHODS

2.1 Experimental apparatus and method

A new experimental test rig was constructed at Institute of Engineering and Energy Technologies at University of the West of Scotland, UK. The main components of the system consist of water cooling circulation system, heating system, test section and data acquisition system. Figure 1 shows the schematic diagram of the experimental apparatus and Figure 2 shows a photo of the overall system.

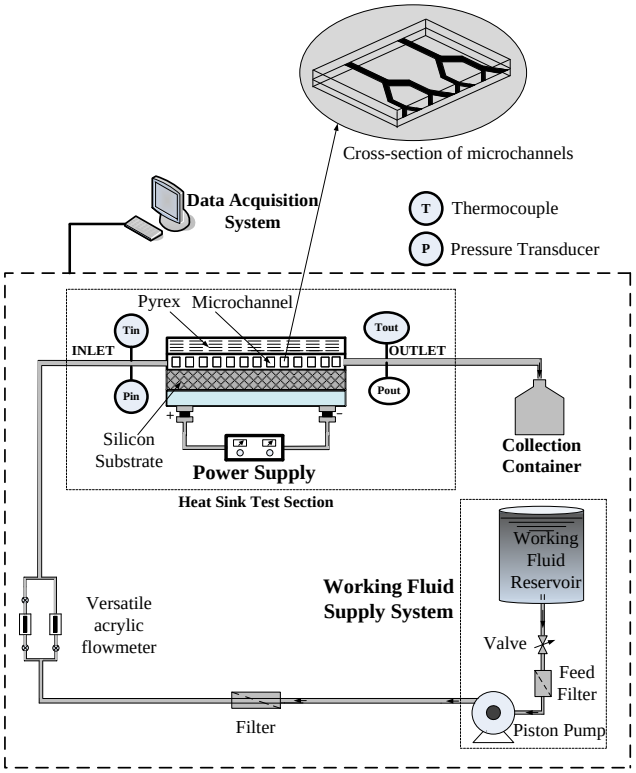

Figure 1. The schematic diagram of the experimental apparatus.

In the water cooling circulation system, the water inlet temperature is controlled by a recirculating digital water bath (SWB23-2, USA) with an accuracy of ±0.2 ℃. Water circulation in the loop is maintained by a peristaltic pump (Watson Marlow Model). A versatile acrylic flowmeter (Cole Palmer) is chosen to provide accurate flow measurement with an accuracy of ±5% FS.

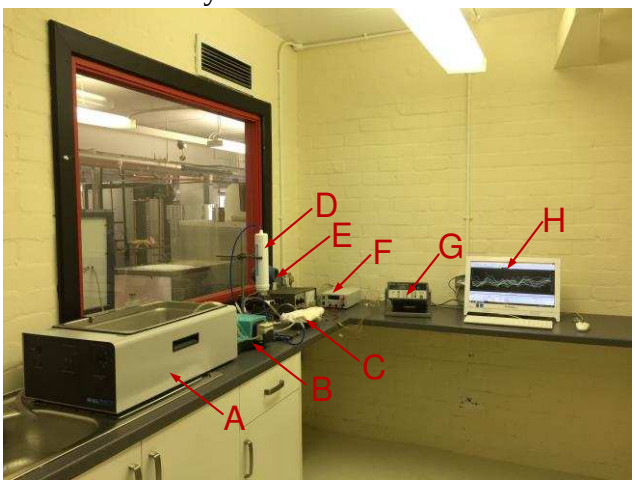

A-Thermal bath, B-Pump, C-Test section, D-Filter, E-Pressure transmitter, F-Power supply, G-Data acquisition, H-Computer.

Figure 2. The overall system including test section.

Figure 3 shows a picture of the designed microchannel that is manufactured using the CNC machine. The copper is selected as the test section material with dimension of 10 cm (W) x 10 cm (H) x 6 mm (D), as shown in Figure 3(a). And the diameter of the microchannel is 1.5 mm. The polyimide film heating element of dimensions 80 mm x 80 mm and 1.52 mm thickness (see Figure 3(b)) that attached to the bottom of the microchannel is connected to a DC power supply (EA-PS 2042-20B) with maximum power output of 300 W to deliver the heating power to the copper. A Rosemount 3051S pressure transmitter (Emerson) with an accuracy of ±0.025% FS is chosen to measure the pressure drop between the inlet and outlet of the test section. In the current study, was is selected as the working fluid.

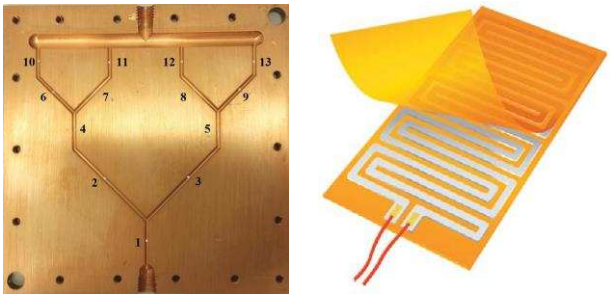

(a) (b)

Figure 3. Microchannel test section (a) and heating element (b).

The test section is instrumented with 13 type K thermocouples which are spot welded directly to the outer surface of the copper wall during each test run. The thermocouples are located at Number 1, 2, …13, as shown in Figure 3 (a). Each thermocouple with an accuracy of ±0.5 ℃ is calibrated prior to testing in order to check and correct for induced temperature bias error that caused by the voltage across the test section. A layer of the glass wool acted as an insulator to minimize the heat losses of the copper plate.

2.2 Data acquisition

The signals measured by the thermocouples are achieved by utilizing Agilent data acquisition system (Model 34970A) and recorded by a computer.

2.3 Experimental procedure

Three typical runs procedure are conducted during the experiment. In the first experiment, keeping the heat flux and water inlet temperature constant, the inlet velocity is changed from 0.6 L/min to 1.0 L/min at an interval of 0.1 L/min. Second experiment is carried out while keeping inlet mass flow rate and inlet temperature constant, but increasing the heat flux from $1.0x10^4$ to $2.5x10^4$ W/m^2. In third set of experiments, mass flow rate and heat flux is kept constant but temperature of flow at the inlet is changed. The experimental conditions are summarized in Table 1.

Table 1. Experimental conditions

Parameter	Unit	Range
Flow rate	L/min	0.6 – 1.0
Heat flux	W/m^2	$1x10^4$ – $2.5x10^4$
Inlet temperature	K	323.15 – 348.15

2.4 Computational model

For comparison and further calculation, the CFD study chose the same geometry of the experimental work outlined above as the computational domain, as shown in Figure 4(a) and Figure 4(b).

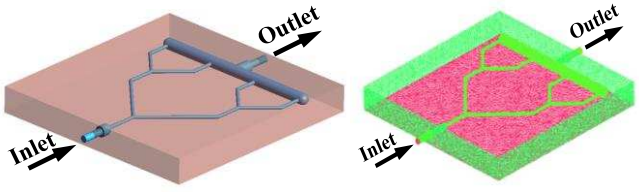

(a) (b)

Figure 4: (a) Geometry and (b) computational domain.

A grid independence study is performed by using different grids and a compromise between computation accuracy and computing capability led to the use of 1.3 million cells. In the current study, a standard k-ε turbulence model is employed. To comply with the experiments, the boundary conditions are set as following: 293 K for the water temperature at inlet of the test section, the mass flow rate is set to be 1.0 L/min, the heat flux at the bottom surface of the test section is $2.5x10^4$ W/m^2, and the other walls are set to be thermally insulated. The outlet is set constant pressure at 1 atm. The simulation is performed using commercial CFD Fluent solver.

3 RESULTS AND DISCSSION

In the following sections, the effects of some typical control parameters, such as mass flow rate and heat flux, on temperature difference across the test section are discussed experimentally. Afterwards, the developed numerical model will be firstly evaluated through the comparison of the temperature drops between the numerical results and the experimental data. Then the flow characteristics and the temperature distribution will be examined as a case study. Finally, a CFD simulation on a new designed MCHS will be discussed based on the developed CFD model.

3.1 Experimental results

Figure 5 shows the variation of the mass flow rate on the temperature difference at steady state. In this study, experiments are done for five different flow rates: 0.6, 0.7, 0.8, 0.9 and 1.0 L/min, and the water temperature and heat flux are kept constant, which are 293 K and $1.0x10^4$ W/m^2, respectively.

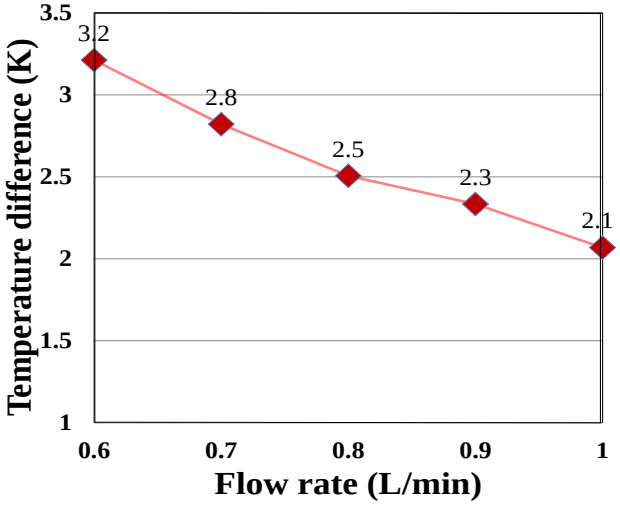

Figure 5: Effect of mass flow rate on temperature difference.

As is expected, the mass flow rate is inversely proportional to change in temperature.

Figure 6 presents the pressure drop across the test section at different flow rates.

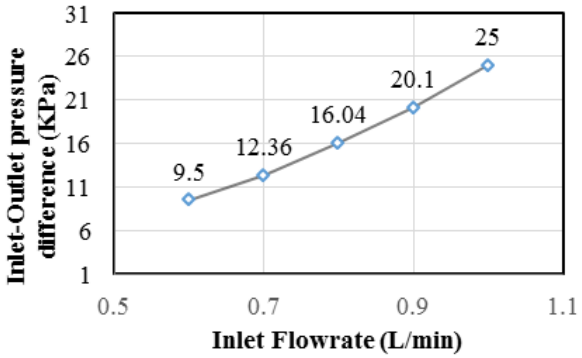

Figure 6: Pressure drop vs flow rate.

It is observed in Figure 6 that the pressure drop increases monotonously with the increase of flow rate. It should be noted that the higher flow rate have a significant effect on the pressure drop. This can be demonstrated that the pressure drop increased from 20.1 KPa at flow rate of 0.9 L/min to 15 KPa at 1.0 L/min, whereas the pressure drop increased from 9.5 KPa at 0.6 L/min to 12.36 KPa at 0.7 L/min.

Figure 7 shows the variation of the temperature difference for heat flux applied from $1.0x10^4$ to $2.5x10^4$ W/m^2 in an increment of $5x10^3$ W/m^2 at fixed mass flow rate of 1.0 L/min.

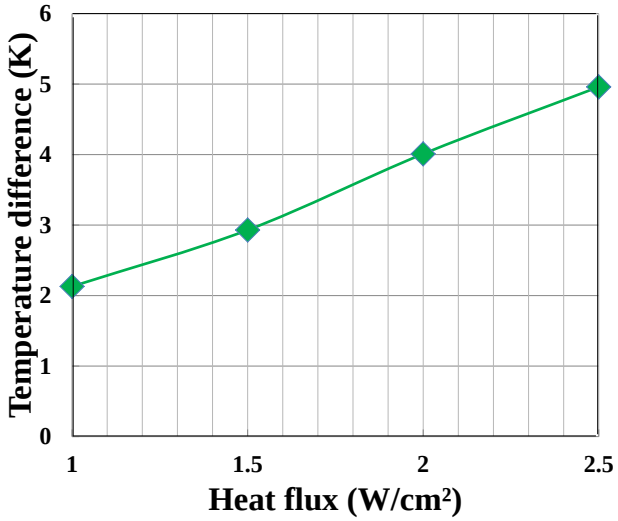

Figure 7: Effect of heat flux on temperature difference.

From Figure 7, it can be seen clearly that the linear nature of relation between change in temperature and heat flux. As the heat flux applied to the heat sink increases, the flowing water through it is able to take more heat away by convection.

The effects of water inlet temperature on the temperature difference across the test section are depicted in Figure 8.

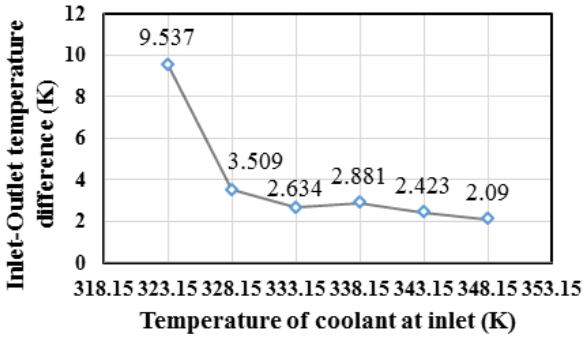

Figure 8: Effect of water inlet temperature on temperature difference.

It can be observed from Figure 8 that as the temperature of coolant at inlet increases, the rate at which heat is carried out of the system decreases. It can be easily understand that lower temperature of coolant has a better effect.

3.2 Model validation

Prior to conducting the aimed computations, it is necessary to validate the computational model. Figure 9 shows the comparison of the temperature difference across the test section between the numerical results and experimental data at five different mass flow rates of 0.6, 0.7, 0.8, 0.9 and 1.0 L/min while the water inlet temperature and heat flux are fixed.

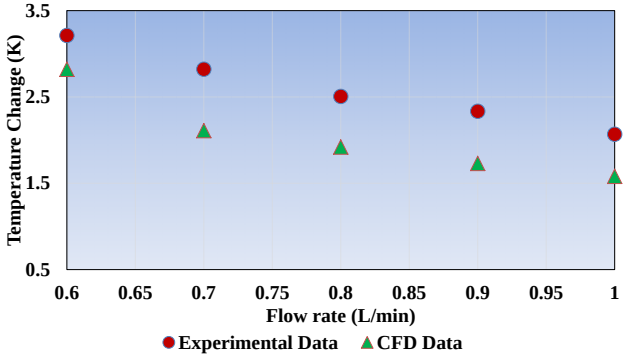

Figure 9: Comparison of computed and measured temperature difference between the inlet and outlet of the test section.

Compared to the experimental data, the computed temperature difference results agree well with the experimental data with an accuracy of less than 1%.

3.3 Flow and heat transfer analysis

It is believed that the fluid flow alters the temperature on the copper plate when a constant heat flux is applied at the bottom. Based on the CFD simulation results, Figure 10 exhibits the profiles of contour temperature, pressure and velocity of the microchannel at steady state when a constant water inlet temperature (293 K), mass flow rare (1.0 L/min) and heat flux ($2.5x10^4$ W/m^2) is applied.

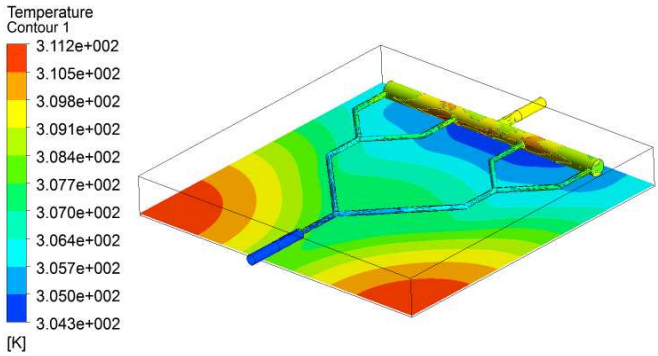

(a) Temperature

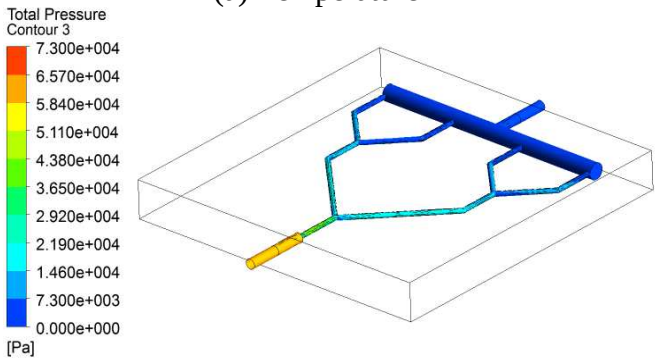

(b) Pressure

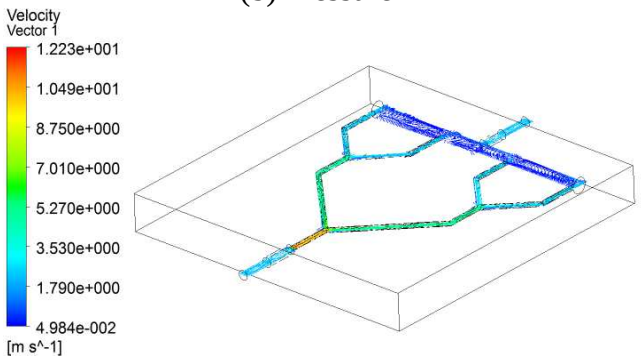

(c) Velocity

Figure 10: (a) Temperature, (b) pressure and (c) velocity profile of the microchannel.

As shown in Figure 10(a), the plate's surface temperature is down close to the channels as the water is dissipating the heat away but some hot spots as observed as the red regions in the Figure. The temperature in plate near the outlet is very low since the presence of comparatively more channels in the region. It is easy to understand from the Figure 10(b) that a high pressure is achieved at the inlet of the test section. As water goes further, the pressure decreases till the atmospheric pressure is achieved. Figure 10(c) indicates that the contour of velocity inside the microchannel. It is clearly seen that the velocity is dominated by the shape of the microchannel.

3.4 Flow & heat transfer of a new design

Efficiency of heat is affected by 'spreading resistence' of any heat sink in a very adverse manner. This resistence is not affected by the shape of heat sink, however even distribution of microchannel can reduce it in a significant manner. A new design of MCHS with more evenly distributed is shown in Figure 11 as the computational domain is illustrated.

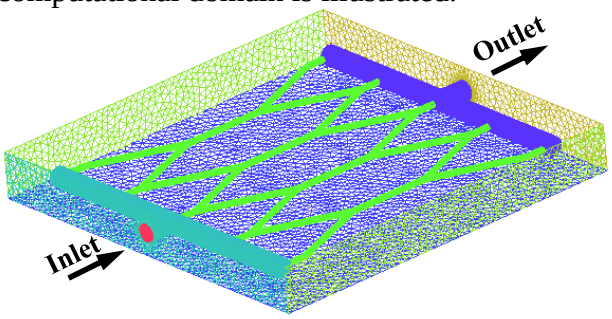

Figure 11: Computational domain.

Figure 12 shows the profiles of contour temperature, pressure and velocity of a new MCHS at steady state when a constant water inlet temperature (293 K), mass flow rare (1.0 L/min) and heat flux ($5.0x10^5$ W/m^2) is applied.

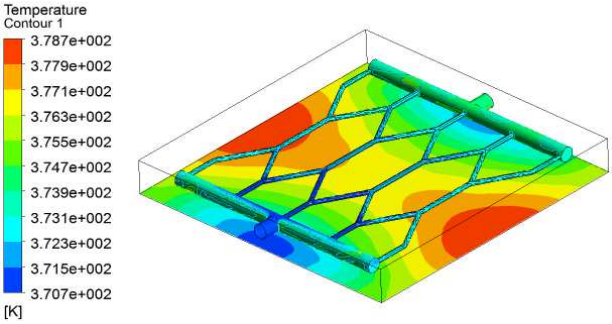

(a) Temperature

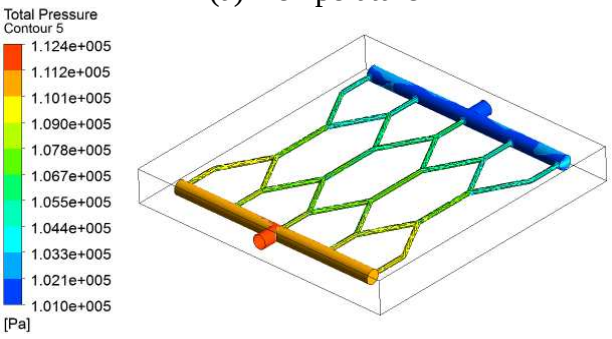

(b) Pressure

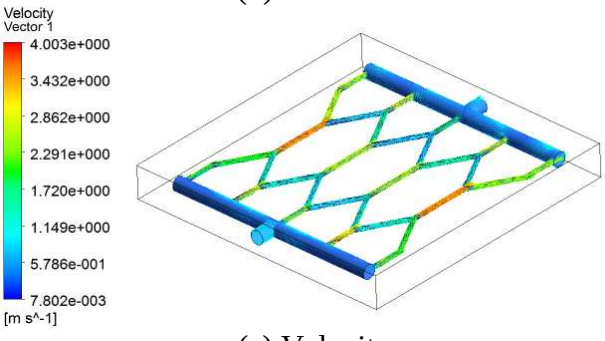

(c) Velocity

Figure 12: (a) Temperature, (b) pressure and (c) velocity profile of a new MCHS.

It is found from Figure 12 (a) that more stable distribution of temperature is achieved for the new design of MCHS. This heat sink design can

be further optimized by reducing the size of microchannels or changing the angle of bifurcation.

4 CONCLUSIONS

A Y-fractal micro channel based heat sink was designed, manufactured and tested to investigate the effects of three different control parameters, i.e. mass flow rate, heat flux and inlet temperature, on the flow and heat transfer characteristics. Validation of the CFD model is carried out through comparison with obtained experimental data. Results show that close agreement is achieved between the computed and experimental results. Further calculation based on the proposed method for a new design of MCHS is numerically well demonstrated.

ACKNOWLEDGEMENTS

The authors gratefully acknowledge the financial support from Royal Society (Grant No. RG130646).

REFERENCES

[1] H. Ganapathy, A. Shooshtari, K. Choo, S. Dessiatoun, M. Alshehhi, M. Ohadi, Volume of fluid-based numerical modelling of condensation heat transfer and fluid flow characteristics in microchannels, International Journal of Heat and Mass Transfer, Vol. 65, pp. 72-72, 2013.

[2] M. Kalteh, A. Abbassi, M. Saffar-Avval, A. Frijns, A. Darhuber, J. Harting, Experimental and numerical investigation of nanofluid forced convection inside a wide microchannel heat sink, Applied Thermal Engineering, Vol. 36, pp. 260-268, 2012.

[3] B. Fani, A. Abbassi, M. Kalteh, Effect of nanoparticles size on thermal performance of nanofluid in a trapezoidal microchannel-heat-sink, International Communications in Heat and Mass Transfer, Vol. 45, pp. 155-161, 2013.

[4] P. Selvakumar, S. Suresh, S. Salyan, Investigations of effect of radial flow impeller type swirl generator fitted in an electronic heat sink and Al_2O_3/water nanofluid on heat transfer enhancement, Chemical Engineering and Processing: Process Intensification, Vol. 72, pp. 103-112, 2013.

[5] J.F. Tullius, Y. Bayazitoglu, Effect of Al_2O_3/H_2O nanofluid on MWNT circular fin structures in a minichannel, International Journal of Heat and Mass Transfer, Vol. 60, pp. 523-530, 2013.

[6] M. Rahimi, E. Karimi, M. Asadi, P. Valeh-e-Sheyda, Heat transfer augmentation in a hybrid microchannel solar cell, International Communications in Heat and Mass Transfer, Vol. 43, pp. 131-137, 2013.

[7] G. L. Morini, Single-phase convective heat transfer in microchannels: a review of experimental results, International Journal of Thermal Sciences, Vol. 43, pp. 631-651, 2004.

[8] M. Asadi, G. Xie, B. Sunden, A review of heat transfer and pressure drop characteristics of single and two-phase microchannels, International Journal of Heat and Mass Transfer, Vol. 79, pp. 34-53, 2014.

[9] Y. Li, F. Zhang, B. Sunden, G. Xie, Laminar thermal performance of microchannel heat sinks with constructal vertical Y-shaped bifurcation plates, Applied Thermal Engineering, Vol. 73, pp. 185-195, 2014.

[10] C. Zhang, Y. Lian, C. Hsu, J. Teng, S. Liu, Y. Chang, R. Greif, Investigations of thermal and flow behaviour of bifurcations and bends in fractal-like microchannel networks: Secondary flow and recirculation flow, International Journal of Heat and Mass Transfer, Vol. 85, pp. 723-731, 2015.

[11] C. Zhang, Y. Lian, X. Yu, W. Liu, J. Teng, T. Xu, C. Hsu, Y. Chang, R. Greif, Numerical and experimental studies on laminar hydrodynamic and thermal characteristics in fractal-like microchannel networks. Part A: Comparisons of two numerical analysis methods on friction factor and Nusselt number, International Journal of Heat and Mass Transfer, Vol. 66, pp. 930-938, 2013.

[12] C. Zhang, Y. Lian, X. Yu, W. Liu, J. Teng, T. Xu, C. Hsu, Y. Chang, R. Greif, Numerical and experimental studies on laminar hydrodynamic and thermal characteristics in fractal-like microchannel networks. Part B: Investigations on the performances of pressure drop and heat transfer, International Journal of Heat and Mass Transfer, Vol. 66, pp. 939-947, 2013.

[13] S. Xu, W. Wang, K. Fang, C. Wong, Heat transfer performance of a fractal silicon microchannel heat sink subjected to pulsation flow, International Journal of Heat and Mass Transfer, Vol. 81, pp. 33-40, 2015.

[14] Y.J. Lee, P.K. Singh, P.S. Lee, Fluid flow and heat transfer investigations on enhanced microchannel heat sink using oblique fins with parametric study, International Journal of Heat and Mass Transfer, Vol. 81, pp. 325-336, 2015.